

Scope and Limitations of the Liebeskind–Srogl Cross-Coupling Reactions Involving the Biellmann BODIPY

Lourdes Betancourt-Mendiola,[†] Ismael Valois-Escamilla,[†] Teresa Arbeloa,[‡] Jorge Bañuelos,^{*,‡} Iñigo López Arbeloa,[‡] Juan O. Flores-Rizo,[†] Rongrong Hu,[§] Erik Lager,[†] César F. A. Gómez-Durán,[†] José L. Belmonte-Vázquez,[†] Mayra R. Martínez-González,[†] Ismael J. Arroyo,[†] Carlos A. Osorio-Martínez,[†] Enrique Alvarado-Martínez,[†] Arlette Urías-Benavides,[†] Brenda D. Gutiérrez-Ramos,[†] Ben Zhong Tang,[§] and Eduardo Peña-Cabrera^{*,†}

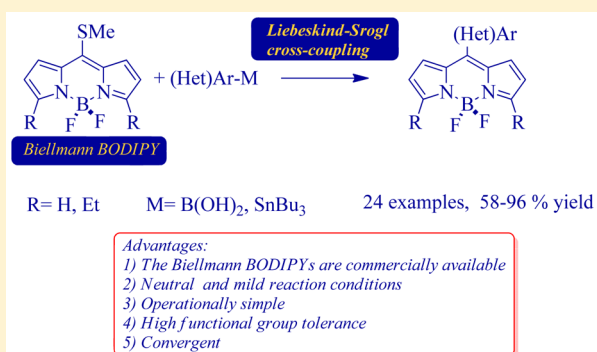
[†]Departamento de Química, Universidad de Guanajuato, Col. Noria Alta S/N, Guanajuato 36050, Mexico

[‡]Departamento de Química Física, Universidad del País Vasco-EHU, Apartado 644, 48080 Bilbao, Spain

[§]Department of Chemistry, The Hong Kong University of Science & Technology, Clear Water Bay, Kowloon, Hong Kong, China

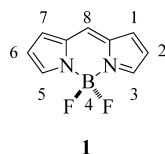
Supporting Information

ABSTRACT: Several new examples of *meso*-(het)arylBODIPY were prepared via the Liebeskind–Srogl (L–S) cross-coupling reaction of the Biellmann BODIPYs (**1a,b**) and aryl- and heteroarylboronic acids in good to excellent yield. It was shown that this reaction could be carried out under microwave heating to shorten reaction times and/or increase the yield. It was illustrated that organostannanes also participate in the L–S reaction to give the corresponding BODIPY analogues in short reaction times and also with good to excellent yields. We analyze the role of the substituent at the sensitive *meso* position in the photophysical signatures of these compounds. In particular, the rotational motion of the aryl ring and the electron donor ability of the anchored moieties rule the nonradiative pathways and, hence, have a deep impact in the fluorescence efficiency.



INTRODUCTION

Truly remarkable applications of dipyrromethene–BF₂ fluorophores **1** (BODIPYs)¹ continue to appear in the literature. These fluorescent compounds were first reported by Treibs and Kreuzer in 1968.² Little did they know the great impact these analogues were to have in so many disciplines. The properties of this family of compounds are reported in excellent reviews.³



Some relevant examples of their applications include the tagging of biomolecules,⁴ as components of supramolecular light-harvesting systems,⁵ in the construction of dye-sensitized solar cells,⁶ as sensors,⁷ as components of fluorescent nanocars,⁸ as nanoparticle conjugates,⁹ as ligands for human β -adrenoceptors,¹⁰ as components of bulk heterojunction solar cells,¹¹ in real-time PCR methods,¹² and as visualizers for Langerhans islets,¹³ and as a quality control in milk,¹⁴ among others.

Assorted methods exist in the literature dealing with the functionalization of the BODIPY 1–7 positions.¹⁵ The importance of *meso*-substituted bodipy analogues was pointed out by Nagano et al.¹⁶ They considered the bodipy general structure as a two-component entity (Figure 1), the bodipy

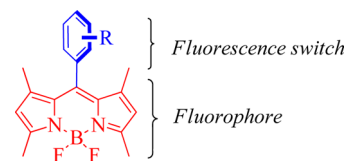


Figure 1. Roles of the fragments of a *meso*-aryl-substituted BODIPY.

portion (in red) as the fluorophore and the aryl moiety (in blue) as the fluorescent switch, that regulates the quantum yields, at least in the 1,7-dimethylbodipy derivatives.

Additionally, the *meso* position is the most sensitive to substituent effects because, upon excitation, an important variation in the electron density takes place at that site.¹⁷ From a strategic point of view, the *meso* position is arguably the most

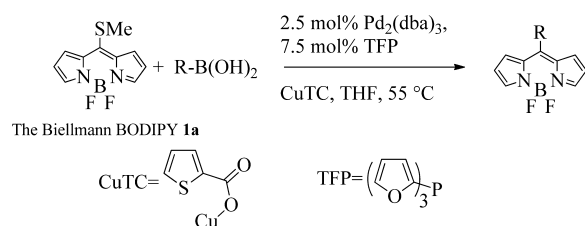
Received: April 2, 2015

Published: May 12, 2015

important because in the majority of the applications that have been devised for BODIPYs it is the position of choice for the attachment of the substrate to study.¹⁸

In the initial contribution of this laboratory,¹⁹ we reported a mild method that allowed the introduction of a series of functional groups at the *meso*-position via the Liebeskind-Srogl (L–S) cross-coupling²⁰ under neutral conditions (Scheme 1).

Scheme 1. Application of the Liebeskind–Srogl Cross-Coupling in the Synthesis of *Meso*-Substituted BODIPY Analogues Using the Biellmann BODIPY 1



The key component of this process was 8-methylthioBODIPY (**1a**), henceforth termed the Biellmann BODIPY.²¹ The

structures of the BODIPY analogues prepared by this methodology (**2–20**) are shown in Chart 1.

In that contribution, the advantages of this methodology over the typical acid-catalyzed condensation of an aldehyde and an excess amount of pyrrole (the Lindsey²² conditions) method were pointed out. Summarizing, the main shortcomings of the Lindsey methodology include a separate synthesis of the starting aldehyde if it is not commercially available, cumbersome purifications, incompatibility of the substituents on the het(aryl) ring of the aldehyde to acidic conditions, oxidation, and strong Lewis acid exposure (BF_3).

In two further contributions that demonstrated the usefulness of boronic acids as partners in the L–S cross-coupling, derivatives of the type **21–24** were prepared.²³

We have also demonstrated that the Biellmann BODIPY (**1**) engages in a desulfurative reduction to give the parent unsubstituted BODIPY dye²⁴ in $\text{S}_{\text{N}}\text{Ar}$ -like processes to displace the 8-methylthio group by amines,²⁵ phenols and alcohols,²⁶ and C-centered soft nucleophiles.²⁷ In a recent contribution, we have shown that carbohydrate-BODIPY hybrids could be prepared in a one-pot sequence that entailed a L–S cross-

Chart 1

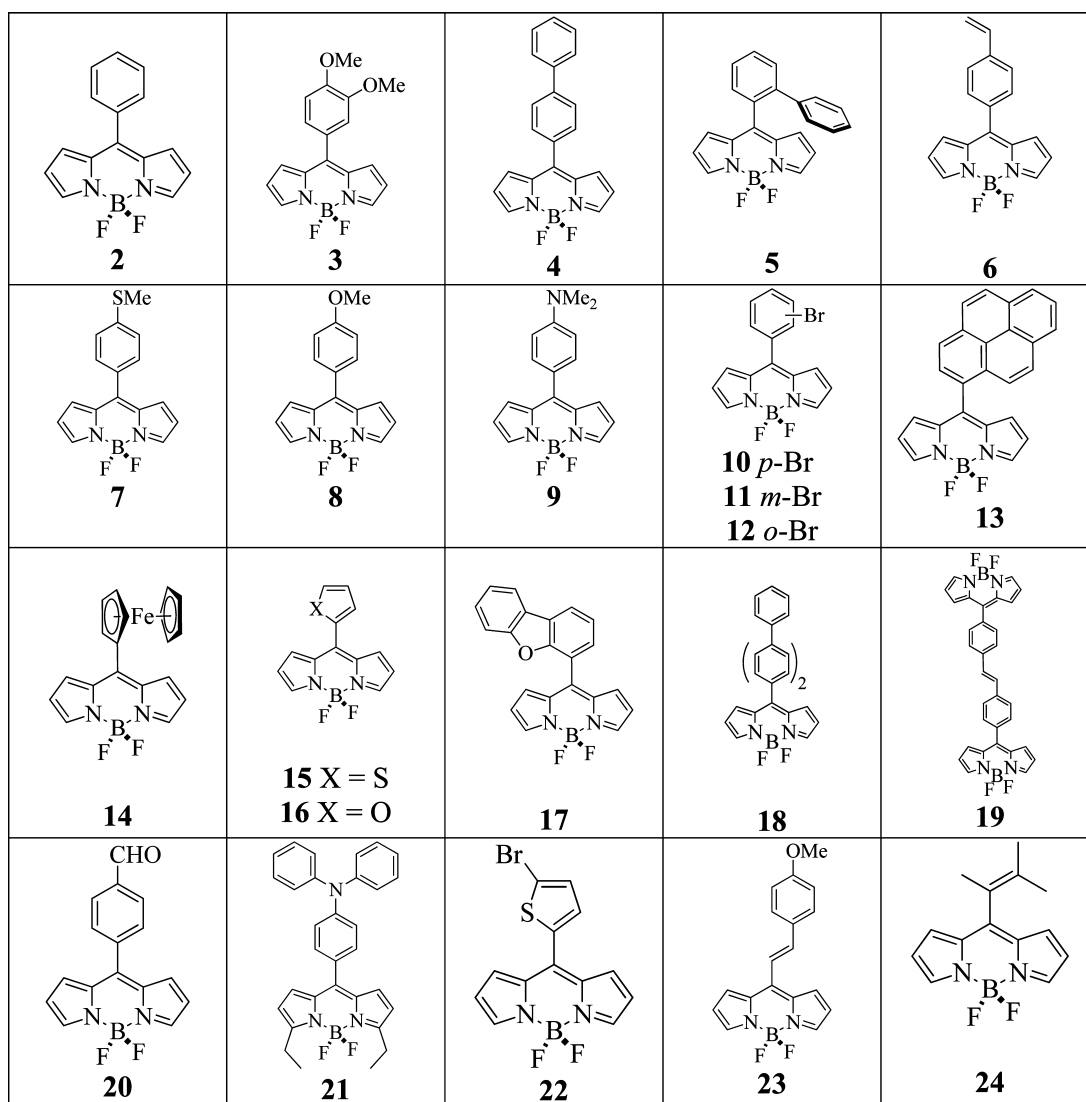
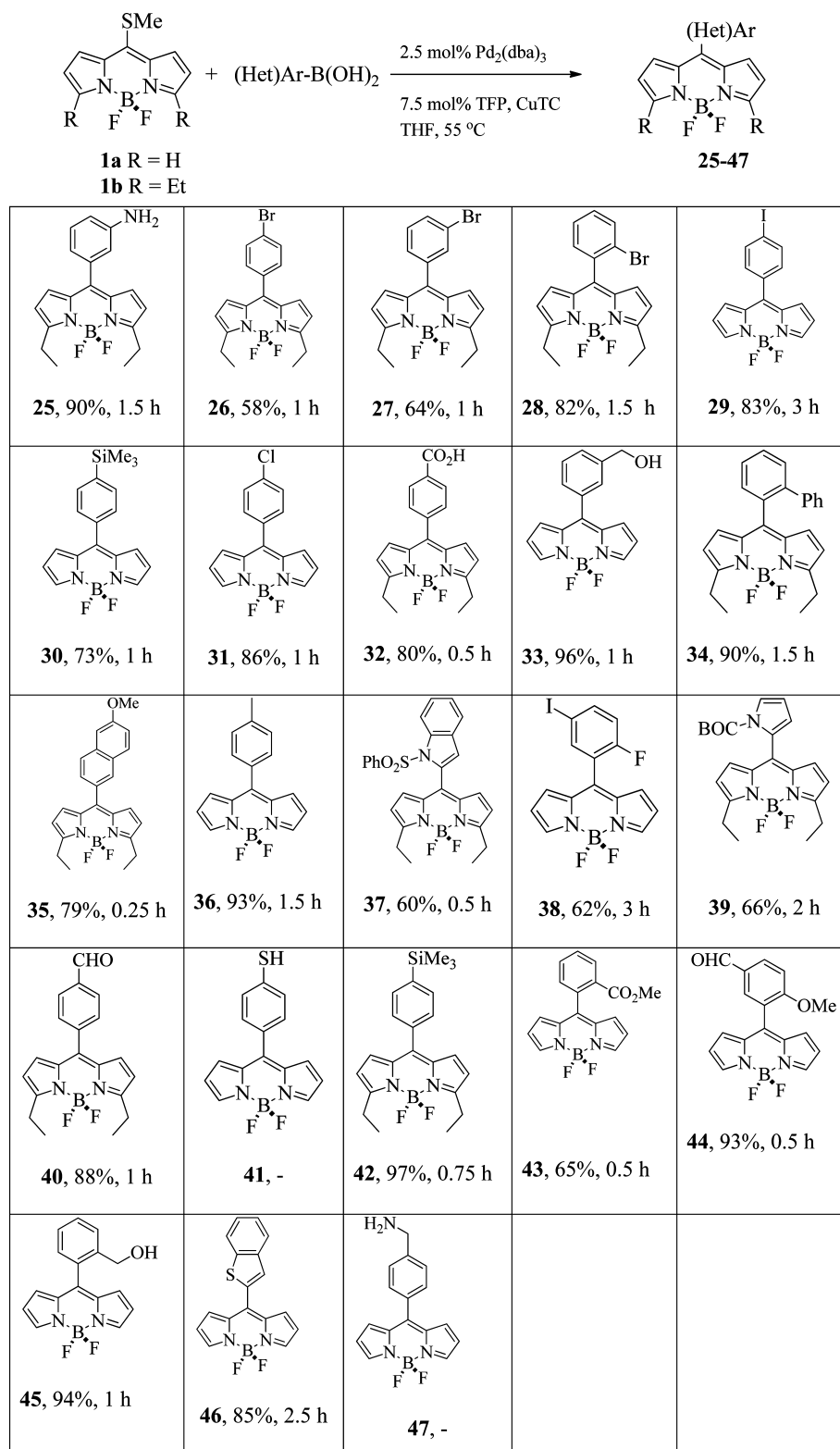


Chart 2. Synthesis of *Meso*-Substituted BODIPY Dyes^a

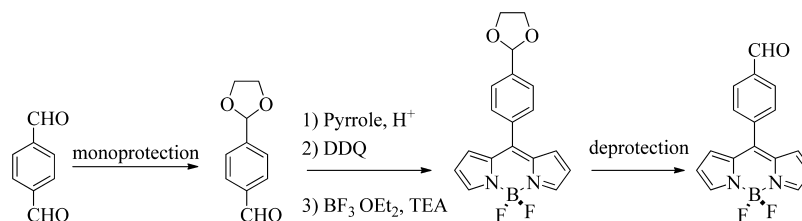
^aIsolated yields. Conditions: **1a** or **1b** (1 equiv), boronic acid (3 equiv), CuTC (3 equiv), Pd₂(dba)₃ (2.5 mol %), TFP (7.5 mol %), THF (3 mL).

coupling followed by a copper-catalyzed azide–alkyne reaction.²⁸

We wish to disclose herein a more in-depth study of the scope and limitations of the Biellmann BODIPY as a participant in cross-coupling reactions leading to the synthesis of *meso*-

substituted BODIPY dyes as well as the optical data of selected examples prepared by this methodology. We seek to demonstrate that both the Biellmann BODIPY (**1a**) and its alkylated analogue **1b** are privileged starting materials for the efficient and straightforward preparation of assorted BODIPY

Scheme 2. Synthesis of 40 Using the Lindsey Method



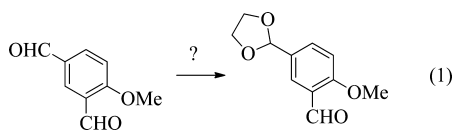
derivatives. The advantages of this process are more relevant since both **1a** and **1b** are now commercially available.

RESULTS AND DISCUSSION

Cross-Couplings with Boronic Acids. Following the reaction conditions showed in Scheme 1, derivatives **25–47** were prepared (Chart 2).

Similar to the results observed in our first contributions,^{19,23b} the LS cross-coupling reaction of the Biellmann BODIPYs **1a,b** with a greater variety of aryl- and heteroarylboronic acids continued to give excellent results. The electronic nature of the arylboronic acids does not affect either the reaction time or the chemical yields. Arylboronic acids with either electron-releasing or electron-withdrawing groups react very smoothly to produce the expected products in good yields. Sterically demanding boronic acids efficiently reacted as well (**28**, **34**, **37**, **38**, **39**, **43**, **44**, and **45**). Arylboronic acids with reactive functional groups smoothly reacted to produce the desired products, i.e., compounds **32**, **33**, and **45** without having to protect them. Heteroarylboronic acids that are known to protodeboronate under Suzuki conditions²⁹ reacted efficiently under the neutral LS cross-coupling reaction conditions to yield compounds **15**, **16**, **37**, **39**, and **46** in good yields and short reaction times. The family of halogen-containing BODIPYs initially reported (**10**, **11**, **12**, and **22**) was now extended to analogues that contain Br, I, and Cl with different substitution patterns that could be further elaborated via transition-metal-catalyzed reactions (**26**, **27**, **28**, **29**, **31**, and **38**). Of particular interest is the straightforward preparation the formylaryl derivatives **40** and **44** in 88 and 93% yield, respectively. If one wanted to prepare **40** using the traditional Lindsey method, several steps involving protection and deprotection would be needed³⁰ (Scheme 2). On the other hand, the same compound could be prepared in a single and efficient operation via the L–S cross-coupling.

Preparation of compound **44**, however, would be lengthy at best using the Lindsey method because it would imply the monoprotection of 4-methoxysophthalaldehyde (eq 1) with its inherent regioselectivity issues.



The numerous examples of commercially available formyl-containing arylboronic acids allows for the preparation of many BODIPY derivatives and their possible applications in areas such as dye-sensitized solar cells,^{30b} the construction of energy-transfer cassettes,^{30c} and cysteine and homocysteine sensors.³¹ 4-(Aminomethyl)phenylboronic acid failed to yield the desired product **47**, presumably because the nucleophilic amino group displaced the MeS group in **1a** faster than the L–S reaction took place.²⁴ This drawback was not observed in the case of 3-

aminophenylboronic acid to give **25** due to the reduced nucleophilicity of the nitrogen atom in aromatic amines. A similar phenomenon may have taken place to prevent the formation of **41**. We recently reported the fast trans-thiolation of **1a** in the presence of arylthiols in THF.³²

L–S Cross-Couplings under Microwave Irradiation. We then decided to explore the efficiency of the microwave irradiation. Thus, a short survey was carried out (Table 1).

Table 1 shows that the L–S cross-coupling reaction is quite compatible with the microwave heating regime. In all cases studied, the reaction times shortened significantly. Although the yields in entries 1 and 2 remained the same, those of entries 3–5 increased. Overall, carrying out the L–S coupling under microwave heating proved advantageous.

Cross-Couplings with Organostannanes. Since organostannanes also participate in the L–S cross-coupling,³³ it was decided to compare their reactivity against that observed with boronic acids.

Initial testing of the typical L–S reaction conditions ($\text{Pd}_2(\text{dba})_3$, TFP, Cu(I)TC, THF, 55 °C) for the coupling of **1a** with organostannanes led to incomplete conversions even after 3 days. One attempt to accelerate the reaction in the presence of 1 equiv of CsF ³⁴ failed; only decomposition of **1a** was observed. The catalytic system was changed to $\text{Pd}(\text{PPh}_3)_4$, which resulted in a rather complex reaction mixture. We then decided to use the conditions reported by Guillaumet et al.³⁵ for similar reactions. The results are shown in Table 2.

Although the products were obtained in moderate to good yields, the reactions in all of the cases analyzed were very sluggish, taking up to 50 h to go to completion.

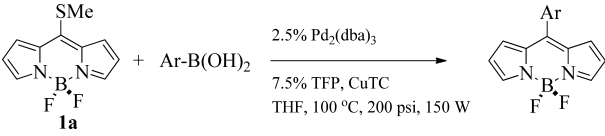
Since the results were not quite satisfactory, we turned our attention to studying the outcome of the reaction using copper(I) diphenylphosphinate, $\text{Cu}(\text{I})\text{OP}(\text{O})\text{Ph}_2$, as the Cu source, since it has been demonstrated that it gives good results in similar cross-coupling with organostannanes.^{33a} The results are shown in Table 3.

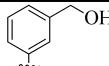
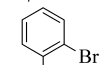
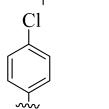
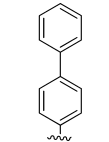
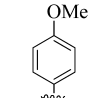
Gratifyingly, the reaction times in all cases surveyed dropped to 1 h or less and the yields increased significantly irrespective of the electronic properties of the aryl groups, at least in the group studied.

Photophysical Properties. The spectroscopic properties of selected *meso*-(het)arylBODIPY derivatives listed in Charts 1 and 2 are collected in Table 4.

The presence of a phenyl ring at the *meso* position of the BODIPY **2** has little impact in the absorption spectra due to the absence of resonance interaction. In fact, the 8-phenyl group does not contribute to the electronic density of the frontier molecular orbitals involved in the electronic transition.¹⁷ Moreover, the functionalization of such a ring scarcely shifts the absorption band (centered around 500–505 nm, Table 4), although electron donors (i.e., amine in **9** and methoxy in **3** and **8**) or acceptors (i.e., halogens in **10–12** or **29** and carboxylates in **32** and **43**) have been grafted to different positions of the 8-

Table 1. L–S Cross-Couplings with Boronic Acids under Microwave Irradiation

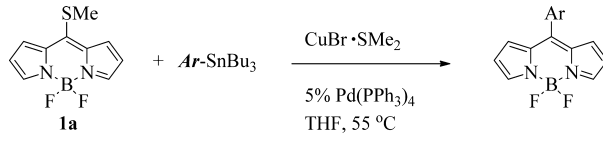


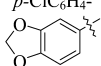
Entry	Ar	Time μw heating	% yield ^a	Time	% yield thermal heating	Compd
1		5 min	95	1 h	96	33
2		30 min	85	70 min ^b	83 ^b	12
3		20 min	90	1 h	86	31
4		10 min	92	5 h ^b	79 ^b	4
5		5 min	91	30 min ^b	76 ^b	8

^aIsolated yields. **1a** (1 equiv), boronic acid (3 equiv), CuTC (3 equiv), Pd₂(dba)₃ (2.5 mol %), TFP (7.5 mol %), THF (3 mL) in a sealed vessel.

^bData taken from ref 18.

Table 2. Survey of the Reactivity of Organostannanes in the Liebeskind–Srogl Cross-Coupling Using the Guillaumet Conditions



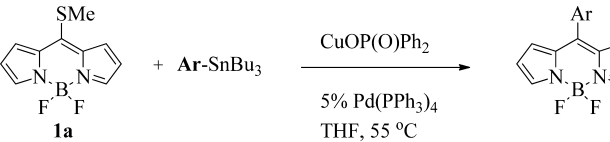
Entry	Ar	time (h)	Compd.	% yield ^a
1	<i>p</i> -CH ₃ OC ₆ H ₄ -	49	8	52
2	<i>p</i> -CH ₃ C ₆ H ₄ -	50	36	75
3	<i>p</i> -ClC ₆ H ₄ -	22	31	79
4		52	48	52
5	C ₆ H ₅ -	46	2	52

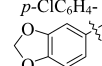
^aIsolated yield. Conditions: BODIPY **1a** (1 equiv), ArSnBu₃ (3 equiv), CuBr·SMe₂ (3 equiv), Pd(PPh₃)₄ (5 mol %), THF (5 mL).

phenyl. Just a slight bathochromic shift (10–15 nm, Table 4) is recorded in the absorption band owing to the direct attachment of electron-donor heteroaryls (thiophene in **15** and **46** or furane in **16**) to the *meso* position of the BODIPY core and at the *ortho* positions of the 8-aryl moiety (compounds **2–20**, except **12** and **17** from Chart 1, and **25–27**, **29–33**, **36**, **40**, **42**, and **46** from Chart 2) are characterized by very low fluorescence efficiency (<10%, Table 4). The rotational motion of the aryl at *meso* position greatly enhances the vibrational coupling with the BODIPY chromophore and eventually can distort its planarity. Both factors result in an increase in the nonradiative relaxation pathways.³⁶ The fluorescence efficiency is worsened by the additional presence in the aryl ring of strong electron-donating or -withdrawing groups which enable fluorescence-quenching intramolecular charge-transfer (ICT) processes. For instance,

Nonetheless, the arylation of the *meso* position plays a fundamental role in the emission signatures (mainly in the fluorescence efficiency) of the herein attained compounds

Table 3. Survey of the Reactivity of Organostannanes in the Liebeskind–Srogl Cross-Coupling Using Cu(I) Phosphinate as Cu(I) Source



Entry	Ar	time (h)	Compd.	% yield ^a
1	<i>p</i> -CH ₃ OC ₆ H ₄ -	1.0	8	85
2	<i>p</i> -CH ₃ C ₆ H ₄ -	0.5	36	77
3	<i>p</i> -ClC ₆ H ₄ -	0.5	31	81
4		0.5	48	75
5	C ₆ H ₅ -	0.5	2	90

^aIsolated yield. Conditions: BODIPY **1a** (1 equiv), ArSnBu₃ (3 equiv), CuOP(O)Ph₂ (3 equiv), Pd(PPh₃)₄ (5 mol %), THF (3 mL).

(Table 4). As a matter of fact, those compounds in which the aryl ring can easily rotate due to the lack of substituents at the adjacent 1 and 7 positions of the BODIPY core and at the *ortho* positions of the 8-aryl moiety (compounds **2–20**, except **12** and **17** from Chart 1, and **25–27**, **29–33**, **36**, **40**, **42**, and **46** from Chart 2) are characterized by very low fluorescence efficiency (<10%, Table 4). The rotational motion of the aryl at *meso* position greatly enhances the vibrational coupling with the BODIPY chromophore and eventually can distort its planarity. Both factors result in an increase in the nonradiative relaxation pathways.³⁶ The fluorescence efficiency is worsened by the additional presence in the aryl ring of strong electron-donating or -withdrawing groups which enable fluorescence-quenching intramolecular charge-transfer (ICT) processes. For instance,

Table 4. Photophysical Properties of Selected BODIPYs in Tetrahydrofuran: Absorption (λ_{ab}) and Fluorescence (λ_{fl}) Wavelengths and Fluorescence Quantum Yield (Φ)^a

compd	λ_{ab} (nm)	λ_{fl} (nm)	% Φ	compd	λ_{ab} (nm)	λ_{fl} (nm)	% Φ ^b
2	501	520	2.6	27	514	533	6.3
3	499	520	1.1	28	518	535	55.0
4	373, 502	524	1.0	29	502	522	0.7
5	493	532	5.3	30	500	519	1.0
6	502	527	0.4	31	502	521	0.7
7	501	524	2.4	32	514	535	2.9
8	498	520	3.5	33	499	516	1.5
9	494	533	0.7	34	516	528	25.0
10	502	527	1.1	35	512	526	5.2
11	504	529	1.3	36	500	516	3.6
12	507	527	29.5	37	517	528	55.4
13	505	533, 622	2.3	38	508	528	8.7
14	506			39	520	533	35.0
15	510	620	2.9	40	516	541	1.7
16	417, 520	583		42	512	529	9.7
17	507	525	13.5	43	502	520	51.0
18	387, 501	524	0.6	44	505	522	43.0
19	503	530		45	500	515	87.8
20	506	539	0.5	46	514		
25	511	526	0.3				
26	502	522	1.3				

^aThe complete photophysical data of compounds listed in Chart 2 are collected in Table S1 (Supporting Information). ^bConcentration: 20 μ M.

the emission becomes almost negligible in compounds **14** and **25** (Table 4), both of them bearing electron-releasing groups (ferrocene and amino, respectively) which are known to be capable of promoting this kind of phenomenon. Moreover, in derivatives **13**, **15**, and **16** even a weak emission from the ICT is detected at long wavelengths, especially with pyrene and thiophene, as shown in Figure 2. Indeed, in compound **13** a dual emission is clearly detected, the fluorescence from the locally excited (LE) state and the fluorescence from the ICT state, which is populated from the LE (Figure 2). The replacement of pyrene by the more electron-donating thiophene (**15**) leads to the complete quenching of the emission from the LE, and just the long wavelength emission

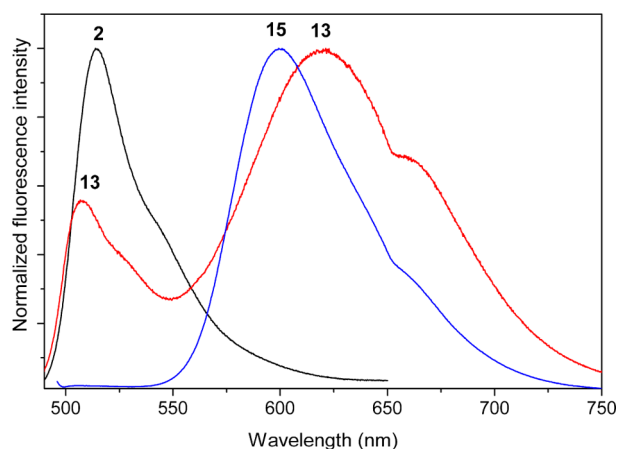


Figure 2. Fluorescence spectra of compounds **2** (8-phenyl), **13** (8-pyrene), and **15** (8-thiophene).

from the ICT is detected, albeit quite weak. It is noteworthy that such red-shifted emission recorded for compound **15** is not longer detected when a phenyl ring is fused to the 8-thiophene **46**, which results in a complete loss of the fluorescence signal. Likely, the charge separation is further favored, increasing the nonradiative deactivation from the ICT state.

As stated above, ethylation at the key chromophoric α -positions not only bathochromically shifts the spectral bands but also counteracts in part the above commented internal conversion promoted by the unconstrained 8-aryl groups. Thus, comparing the analogues bearing the trimethylsilyl group (**30** vs **42**), an improvement in the fluorescence efficiency is attained upon alkylation (from 1% to 9.7% respectively, Table 4). The same trend is nicely observed in the BODIPYs bearing brominated phenyls at different positions (nonalkylated **10**, **11** and **12** vs **26**, **27** and **28** ethylated at positions 3 and 5). Such improvement is attributed to an enhancement in the electronic delocalization by the insertion of inductive electron-donor alkyl groups at the α -positions of the cyanine π -system.³⁶ In fact, the highest molar absorption coefficients (around 90000–100000 $M^{-1} cm^{-1}$ in Table S1, Supporting Information) are calculated for alkylated compounds (i.e., **25**, **27**, **35**, and **42**).

In contrast, the *ortho* substitution of the aryl ring reverses the situation, and bright BODIPYs are attained (Table 4). Figure 3

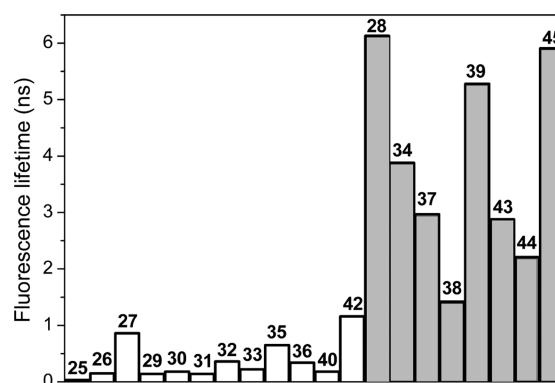


Figure 3. Fluorescence lifetime of selected BODIPY listed in Chart 2 with *ortho*-substitution (gray) and without substitution (white) at such positions of the 8-aryl. For the last set of compounds, the main lifetime (contribution >98%) is provided due to the biexponential deconvolution of the decay curve.

shows that whereas for the aforementioned derivatives with unconstrained 8-aryl and hence low fluorescence quantum yields the lifetimes were very fast (multiexponentials with main lifetime below 1 ns, see Figure 3 and Table S1, Supporting Information), the steric hindrance provided by the *ortho* substitution not only raises the fluorescence efficiency but also lengthens the lifetime (monoexponentials with values around 3–6 ns, those typical of BODIPY, see Figure 3 and Table S1, Supporting Information) owing to the restriction of the aryl free motion. Indeed, among the compounds in Chart 1, the highest fluorescence quantum yield is recorded for compound **12** (29.5% in Table 4) bearing an *ortho*-brominated 8-phenyl fragment, while its brominated analogues at the *para* or *meta* positions (**10** and **11**, respectively) show much more reduced fluorescence efficiencies (1.1% and 1.3%, Table 4). Nicely, the selective bromination of the phenyl ring leads to the same trend in derivatives **26**–**28** from Chart 2, but with ameliorated fluorescence efficiencies due to the aforementioned alkylation effect. Moreover, in Chart 2 all of the -substituted derivatives

(34, 37–39, and 43–45) provide the highest fluorescence efficiencies, which reach values as high as 87.8% for compound 45 (Table 4), and longer lifetimes (gray shaded in Figure 3).

All this background prompted us to analyze the rotational barrier of the 8-phenyl in BODIPYs where its motion is readily free (compound 31 was chosen as representative) or progressively hindered by steric hindrance due to the *ortho* substitution of the aryl groups (38 and 45, those with the smallest and highest fluorescence efficiency among these kind of derivatives). Such a theoretical potential energy surface was computed by scanning and relaxing the energy with regard to the dihedral angle between the phenyl and the indacene core planes using molecular mechanics (MM2) (some representative curves are depicted in Figure 4) and the density functional

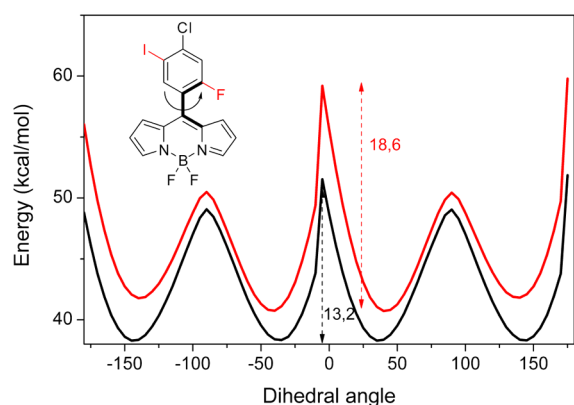


Figure 4. Energy potential surface with regard to the rotation of the 8-aryl fragment by MM2 method for representative compounds 31 and 38.

method (DFT, in particular B3LYP, see the Experimental Section for further details). As expected, the lowest rotational barrier is calculated for compound 31 (13.2 kcal/mol by MM2, Figure 4, and 10.0 kcal/mol by DFT), where the most stable conformation is with the phenyl ring twisted around 52° with respect to the indacene core. The presence of a fluorine atom at the *ortho* position in 38 hinders the phenyl motion as reflected in a higher rotational barrier (18.6 kcal/mol by MM2, Figure 4, and 15.7 kcal/mol by DFT) and a higher twisting angle (60°). However, owing to its small size, the steric hindrance seems not to be high because its fluorescence efficiency is still low (8.7%, Table 4). Further evidence is provided by compound 12 bearing an *o*-bromine. Its larger size should induce a higher steric hindrance to the phenyl motion, reflected in a higher rotational barrier (28.1 kcal/mol by MM2 and 25.1 kcal/mol by DFT) and a more twisted 8-phenyl (65°), which leads to an improved fluorescence signal (29.5% Table 4). In line with this argument, compound 45 shows a larger rotational barrier (around 35 kcal/mol by MM2 and 37.6 by DFT) and a more perpendicular disposition (phenyl twisted 70°). Thus, the geometrical constraint provided by the hydroxymethylene seems to be high enough to lock the phenyl ring motion, thereby giving rise to very high fluorescence efficiencies (up to 87.8%, Table 4). Similar energy values have been reported for the rotational barrier of structurally related 8-aryl-BODIPYs.³⁷ It is noteworthy that the low-demand (from a computationally point of view) and fast MM2 method describes in a qualitative way the evolution of the rotational barrier with regard to the steric hindrance induced by the *ortho* substitution, although the energy values deviate around 3 kcal/mol (usually MM2

overestimates the barrier) with regard to the more accurate DFT method.

Therefore, constrained structures are required to keep the excellent fluorescence signal from the BODIPY. Nevertheless, those derivatives bearing 8-aryl with free motion are applied in the emerging field of molecular rotors to monitor the environmental viscosity owing to the sensibility of both the fluorescence efficiency and lifetime to the ring rotation.³⁸ The set of derivatives presented here could be applied as such probes with the additional advantage that the functionalization of the 8-aryl group (i.e., halogens, carboxylic acids) enables subsequent synthetic modification to improve, for instance, the biological compatibility or to seek a specific target.

CONCLUSIONS

A detailed study has been carried out regarding the scope and limitations of the Biellmann BODIPY as the electrophilic partner in the Liebeskind–Srogl cross-coupling reaction. Several highly substituted aryl- and heteroarylboronic acids were tested to give the desired products with short reaction times and good to excellent yields. The only observed limitations were the cases where the boronic acids contained nucleophilic groups (i.e., NH_2 and SH groups). In those cases, the reaction failed to yield the expected product. It was also demonstrated that the L–S cross-coupling reaction works efficiently using microwaves, giving the products in higher yields, shorter reaction times, or both. In addition to boronic acids, we showed that organostannanes were also effective partners in the L–S cross-coupling reaction with the Biellmann BODIPY. It is envisioned that this methodology will be highly favored by the chemistry community interested in BODIPY dyes due to all of the advantages it presents, as well as because Biellmann BODIPYs are commercially available. The functionalization at the key *meso* position severely alters the fluorescence signatures of the BODIPY. Bulky substituents at the *ortho* position of 8-aryl groups are required to provide high enough steric hindrance, as reflected in higher rotational barriers, to lock the ring rotational motion and ensure high fluorescence efficiencies, which can be further boosted by alkylation at positions 3 and 5. Alternatively, the electron coupling of electron-releasing groups at the 8 position of BODIPY promotes ICT states with long-wavelength emission but with the handicap of its inherent low fluorescence efficiency.

EXPERIMENTAL SECTION

Synthesis and Characterization. All of the starting materials were purchased from commercial sources and used without further purification. ^1H and ^{13}C NMR spectra were recorded on a spectrometer in deuteriochloroform (CDCl_3) with either tetramethylsilane (TMS) (0.00 ppm ^1H , 0.00 ppm ^{13}C) or chloroform (7.26 ppm ^1H , 77.00 ppm ^{13}C) as internal reference. Data are reported in the following order: chemical shift in ppm, multiplicities (br (broadened), s (singlet), d (doublet), t (triplet), q (quartet), sex (sextet), hep (heptet), m (multiplet), exch (exchangeable), app (apparent)), coupling constants, J (Hz), and integration. Infrared peaks are reported (cm^{-1}) with the following relative intensities: s (strong, 67–100%), m (medium, 40–67%), and w (weak, 20–40%). HRMS were recorded as specified. Melting points were determined on the appropriate equipment and are not corrected. TLC was conducted on silica gel on TLC Al foils. Detection was done by UV light (254 or 365 nm). The reactions with microwave heating were carried out on a CEM Discover SP reactor with a vertical IR-focalized internal

temperature sensor. Mass spectrometry data were collected on a TOF analyzer.

Spectroscopic Measurements. The photophysical properties were registered in diluted solutions (around 2×10^{-6} M) of tetrahydrofuran using quartz cuvettes with an optical pathway of 1 cm. UV–vis absorption and fluorescence spectra were recorded on a spectrophotometer and a spectrofluorimeter, respectively. The fluorescence quantum yield (Φ) was obtained by using a suitable commercial BODIPY as reference (PM567 in methanol $\Phi = 0.91$). Radiative decay curves were registered with the time-correlated single-photon counting technique equipped with a microchannel plate detector of picosecond time resolution (20 ps). Fluorescence emission was monitored at the maximum emission wavelength after excitation at 470 nm by means of a diode laser with 150 ps fwhm pulses. The fluorescence lifetime (τ) was obtained after the deconvolution of the instrumental response signal from the recorded decay curves by means of an iterative method. The goodness of the exponential fit was controlled by statistical parameters (χ^2 , Durbin–Watson, and analysis of the residuals). The amplitude average lifetime was calculated by means of $\langle \tau \rangle_{aa} = \sum A_i \tau_i$.

Computational Modeling. Ground-state energy minimizations were performed using the Becke's three-parameter (B3LYP) density functional (DFT) method. The basis set was the double-valence 6-31g, except from those compounds bearing iodine (i.e., **38**) where the lanl2dz basis set, especially parametrized for such heavy atoms, was considered. The optimized geometry was taken as an energy minimum using frequency calculations (no negative frequencies). Rotational energy barriers were calculated from the potential energy surface, which was simulated by relaxed scans of the 8-phenyl twist with regard to the plane of the BODIPY core. Two complementary approaches were considered for this aim. First, the relaxed scans were carried out using the MM2 force field as implemented in ChemBio 3D Ultra (ChemBioOffice 2014 software). The resolution of the scan was 1° . Finally, the potential surface was simulated by the B3LYP method computing and minimizing the energy in steps of 10° . The solvent effect (tetrahydrofuran) was considered in the DFT calculations by the polarizable continuum model (PCM), except for compound **38**, where the calculations were done at the gas phase since the iodine atom is not parametrized in PCM. All of the DFT calculations were performed in Gaussian 09 using the "arina" computational resources provided by the UPV-EHU.

General Procedure for the L–S Cross-Coupling with Boronic Acids (GP1). A Schlenk tube equipped with a stir bar was charged with either **1a** or **1b** (1 equiv), the corresponding boronic acid (3 equiv), and dry THF (3 mL). The mixture was sparged with N_2 for 5 min, whereupon $Pd_2(dba)_3$ (2.5 mol %), trifurylphosphine (7.5%), and CuTC (3 equiv) were added under N_2 . The Schlenk tube was then immersed in a preheated oil bath at $55^\circ C$. The oil bath was removed after the starting BODIPY was consumed (TLC, 20% EtOAc/hexanes) (see Chart 2 for reaction times). After the mixture reached rt, the crude material was adsorbed in SiO_2 gel, and the product was purified by flash chromatography on SiO_2 gel using EtOAc/hexanes as gradient. For the purpose of characterization, the products were crystallized from CH_2Cl_2 /petroleum ether.

BODIPY 25. According to GP1 using **1b** (30.0 mg, 0.102 mmol), 3-aminophenylboronic acid (47.4 mg, 0.306 mmol), $Pd_2(dba)_3$ (2.4 mg, 2.6×10^{-3} mmol), TFP (1.8 mg, 7.6×10^{-3} mmol), and CuTC (58.3 mg, 0.306 mmol). The desired product (26.2 mg, 90% mmol) was obtained as orange crystals. TLC (30% EtOAc/hexanes, $R_f = 0.46$). Mp: 176–177 $^\circ C$. IR (KBr, cm^{-1}): 3495 (m), 3466 (m), 3399 (m), 3377 (m), 2927 (m), 1556 (s), 1432 (s), 1284 (s), 1150 (s), 1031 (s), 998 (s), 950 (s), 800 (s). 1H NMR (200 MHz, $CDCl_3$): δ 7.21 (d, $J = 8.0$ Hz, 2H), 6.89–6.80 (m, 4H), 6.33 (d, $J = 4$ Hz, 2H), 3.79 (bs, 2H), 3.07 (q, $J = 8.0$ Hz, 4H), 1.34 (t, $J = 8.0$ Hz, 6H). ^{13}C NMR (50 MHz, $CDCl_3$): δ 163.3, 146.1, 143.2, 135.2, 134.2, 130.5, 129.0, 120.9, 117.1, 116.7, 116.4, 22.0, 12.8. HRMS FABS ($M + H^+$) calcd for $C_{19}H_{21}BF_2N_3$ 340.1796, found 340.1799.

BODIPY 26. According to GP1 using **1b** (30.0 mg, 0.102 mmol), *p*-bromophenylboronic acid (62.0 mg, 0.306 mmol), $Pd_2(dba)_3$ (2.4 mg, 2.6×10^{-3} mmol), TFP (1.8 mg, 7.6×10^{-3} mmol), and CuTC (58.3

mg, 0.306 mmol). The desired product (23.4 mg, 58%) was obtained as red crystals. TLC (15% EtOAc/hexanes, $R_f = 0.64$). Mp: 135–136 $^\circ C$. IR (KBr, cm^{-1}): 2977 (w), 2941 (w), 1571 (s), 1554 (s), 1488 (s), 1437 (s), 1322 (s), 1257 (s), 1220 (m), 1129 (s), 1070 (m), 1051 (s), 1009 (s), 980 (s), 883 (m), 803 (m), 758 (m), 733 (m). 1H NMR (200 MHz, $CDCl_3$): δ 7.63 (dd, $J_1 = 6.4$ Hz, $J_2 = 2.0$ Hz, 2H), 7.37 (dd, $J_1 = 6.6$ Hz, $J_2 = 2.0$ Hz, 2H), 6.70 (d, $J = 4.4$ Hz, 2H), 6.36 (d, $J = 4.2$ Hz, 2H), 3.07 (q, $J = 7.6$ Hz, 4H), 1.34 (t, $J = 7.6$, 6H). ^{13}C NMR (50 MHz, $CDCl_3$): δ 164.3, 141.4, 134.2, 133.3, 132.0, 131.7, 130.4, 124.6, 117.8, 22.3, 12.9. HRMS FABS ($M + H^+$): calcd for $C_{19}H_{19}BBBrF_2N_2$ 403.0793, found 403.0797.

BODIPY 27. According to GP1 using **1b** (20.0 mg, 0.068 mmol), 3-bromophenylboronic acid (50.0 mg, 0.204 mmol), $Pd_2(dba)_3$ (1.5 mg, 1.7×10^{-3} mmol), TFP (1.2 mg, 5.0×10^{-3} mmol), and CuTC (38.8 mg, 0.204 mmol). The desired product (17.5 mg, 64%) was obtained as an orange solid. TLC (15% EtOAc/hexanes, $R_f = 0.62$). Mp: 124–126 $^\circ C$. IR (KBr, cm^{-1}): 2968 (w), 2939 (w), 1574 (s), 1550 (s), 1488 (s), 1432 (s), 1342 (m), 1320 (s), 1280 (s), 1152 (s), 1139 (s), 1089 (m), 1058 (m), 1039 (s), 985 (s), 899 (m), 798 (m), 761 (m), 733 (m), 720 (m); 1H NMR (200 MHz, $CDCl_3$): δ 7.69–7.650 (m, 2H), 7.46–7.27 (m, 2H), 6.73 (d, $J = 4.4$ Hz, 2H), 6.37 (d, $J = 4.2$ Hz, 2H), 3.09 (q, $J = 7.5$ Hz, 4H), 1.35 (t, $J = 7.6$, 6H); ^{13}C NMR (50 MHz, $CDCl_3$): δ 164.4, 140.8, 136.3, 134.2, 133.1, 133.1, 130.4, 129.9, 129.1, 122.5, 117.9, 22.3, 12.9. HRMS FABS ($M + H^+$) Calcd for $C_{19}H_{19}BBBrF_2N_2$: 403.0793. Found: 403.0798.

BODIPY 28. According to GP1 using **1b** (17.8 mg, 0.066 mmol), *o*-bromophenylboronic acid (39.7 mg, 0.198 mmol), $Pd_2(dba)_3$ (1.5 mg, 1.6×10^{-3} mmol), TFP (1.1 mg, 4.9×10^{-3} mmol), and CuTC (37.6 mg, 0.198 mmol). The product (20.0 mg, 82%) was obtained as red crystals. TLC (15% EtOAc/hexanes, $R_f = 0.52$). Mp: 111–113 $^\circ C$. IR (KBr, cm^{-1}): 3118 (w), 3063 (w), 2979 (w), 2961 (w), 2932 (w), 2872 (w), 1566 (s), 1555 (s), 1490 (m), 1462 (m), 1435 (m), 1345 (w), 1309 (m), 1284 (s), 1212 (w), 1140 (s), 1212 (w), 1140 (s), 1087 (m), 1025 (s), 1000 (s), 982 (s), 885 (w), 796 (m), 746 (m), 736 (m), 704 (w). 1H NMR (400 MHz, $CDCl_3$): δ 7.69 (d, $J = 7.7$ Hz, 1H), 7.45–7.31 (m, 3H), 6.52 (d, $J = 4.2$ Hz, 2H), 6.32 (d, $J = 4.2$ Hz, 2H), 3.08 (q, $J = 7.6$ Hz, 4H), 1.35 (t, $J = 7.6$ Hz, 6H). ^{13}C NMR (100 MHz, $CDCl_3$): δ 165.0, 140.8, 135.5, 134.8, 133.5, 132.0, 131.1, 130.2, 127.2, 123.5, 117.9, 117.8, 21.3, 12.3. HRMS FABS ($M + H^+$): calcd for $C_{19}H_{19}BBBrF_2N_2$ 403.0793, found 403.0798.

BODIPY 29. According to GP1 using **1a** (20.0 mg, 0.084 mmol), *p*-iodophenylboronic acid (62.5 mg, 0.252 mmol), $Pd_2(dba)_3$ (1.9 mg, 2.1×10^{-3} mmol), TFP (1.6 mg, 6.3×10^{-3} mmol), and CuTC (48 mg, 0.252 mmol). The desired product (27.1 mg, 83%) was obtained as an orange solid. TLC (30% EtOAc/hexanes, $R_f = 0.45$). Mp: 193–195 $^\circ C$. IR (KBr, cm^{-1}): 3106 (w), 1563 (s), 1538 (s), 1478 (m), 1414 (s), 1395 (s), 1260 (s), 1224 (m), 1155 (m), 1116 (s), 1082 (s), 976 (m), 908 (m), 774 (m), 739 (m). 1H NMR (200 MHz, $CDCl_3$): δ 7.95 (s, 2H), 7.89 (d, $J = 8.4$ Hz, 2H), 7.30 (d, $J = 8.4$ Hz, 2H), 6.91 (d, $J = 3.6$ Hz, 2H), 6.56 (d, $J = 3.6$ Hz, 2H). ^{13}C NMR (50 MHz, $CDCl_3$): δ 144.7, 137.9, 134.7, 133.3, 132.0, 131.47, 119.0, 118.94, 97.64. HRMS FABS ($M + H^+$): calcd for $C_{15}H_{11}BF_2IN_2$ 395.0028, found 395.0021.

BODIPY 30. According to GP1 using **1a** (50.0 mg, 0.210 mmol), 4-(trimethylsilyl)phenylboronic acid (122.0 mg, 0.630 mmol), $Pd_2(dba)_3$ (4.8 mg, 5.2×10^{-3} mmol), TFP (3.6 mg, 1.6×10^{-3} mmol), and CuTC (119.7 mg, 0.630 mmol). The desired product (52.4 mg, 73%) was obtained as an orange solid. TLC (30% EtOAc/hexanes, $R_f = 0.83$). Mp: 158–159 $^\circ C$. 1H NMR (400 MHz, $CDCl_3$): δ 7.95 (s, 2H), 7.61 (dd, $J = 49.5$, 8.0 Hz, 4H), 6.97 (d, $J = 4.1$ Hz, 2H), 6.55 (d, $J = 3.2$ Hz, 2H), 0.34 (s, 9H).³⁹

BODIPY 31. According to GP1 using **1a** (10.0 mg, 0.042 mmol), 4-chlorophenylboronic acid (19.7 mg, 0.126 mmol), $Pd_2(dba)_3$ (1.0 mg, 1.0×10^{-3} mmol), TFP (0.7 mg, 1.0×10^{-3} mmol), and CuTC (23.9 mg, 0.126 mmol). The desired product (10.9 mg, 86%) was obtained as an orange-reddish solid. TLC (15% AcOEt/hexanes $R_f = 0.36$). Mp: 199–200 $^\circ C$. IR (KBr, cm^{-1}): 3134 (w), 3107 (w), 1572 (s), 1543 (s), 1413 (s), 1401 (s), 1384 (s), 1260 (s), 1155 (m), 1116 (s), 1081 (s), 1049 (m), 979 (m). 1H NMR (200 MHz, $CDCl_3$): δ 7.96 (s, 2H), 7.51 (s, 4H), 6.92–6.90 (m, 2H), 6.57–6.55 (m, 2H). ^{13}C NMR (50 MHz,

CDCl₃): δ 145.9, 144.7, 137.5, 134.9, 132.4, 131.9, 131.5, 129.1, 119.0. HRMS FABS (M + H⁺): calcd for C₁₅H₁₁BClF₂N₂ 303.0672, found 303.0674.

BODIPIY 32. According to GP1 using **1b** (40 mg, 0.136 mmol), 4-carboxyphenylboronic acid (68.0 mg, 0.408 mmol), Pd₂(dba)₃ (3.0 mg, 3.4 × 10⁻³ mmol), TFP (3.0 mg, 0.011 mmol), and CuTC (78.0 mg, 0.411 mmol). The desired product (40 mg, 80%) was obtained as a red solid. TLC (15% EtOAc/hexanes, R_f = 0.33). Mp: 202–203 °C. IR (KBr, cm⁻¹): 2974 (m), 1710 (s), 1575 (s), 1555 (s), 1438 (s), 1275 (s), 1140 (s), 1034 (m), 886 (w), 801 (w), 723 (m), 541 (m); ¹H NMR (200 MHz, CDCl₃): δ 8.23 (d, J = 8.0 Hz, 2H), 7.62 (d, J = 8.0 Hz, 2H), 6.70 (d, J = 4.0 Hz, 2H), 3.07 (q, J = 7.0 Hz, 4H), 1.35 (t, J = 7.5 Hz, 6H). ¹³C NMR (50 MHz, CDCl₃): δ 164.2, 142.8, 138.3, 135.0, 134.3, 132.9, 132.6, 131.2, 129.2, 118.6, 22.6, 13.3. HRMS FABS (M + H⁺): calcd for C₂₀H₂₀BF₂N₂O₂ 369.1586, found 369.1589.

BODIPIY 33. According to GP1 using **1a** (50.0 mg, 0.210 mmol), 3-(hydroxymethyl)phenylboronic acid (95.7 mg, 0.630 mmol), Pd₂(dba)₃ (5.0 mg, 5.3 × 10⁻³ mmol), TFP (3.7 mg, 1.6 × 10⁻³ mmol), and CuTC (119.7 mg, 0.630 mmol). The desired product (60.1 mg, 96%) was obtained as a red solid. TLC (30% EtOAc/hexanes, R_f = 0.17). Mp: 121–123 °C. IR (KBr, cm⁻¹): 3400 (s), 2892 (m), 1545 (s), 1476 (m), 1414 (s), 1389 (s), 1260 (s), 1190 (m), 1116 (s), 1081 (s), 991 (m), 775 (m), 736 (m), 607 (w), 583 (w); ¹H NMR (500 MHz, CDCl₃): δ 7.95 (s, 2H), 7.55 (ddd, J = 21.0, 14.1, 7.5 Hz, 4H), 6.93 (d, J = 3.7 Hz, 2H), 6.55 (d, J = 3.0 Hz, 2H), 4.82 (s, 2H). ¹³C NMR (75 MHz, CDCl₃): δ 147.5, 144.5, 141.7, 134.3, 131.9, 129.9, 129.4, 129.0, 128.9, 118.8, 64.9. HRMS FABS (M + H⁺): calcd for C₁₆H₁₄BF₂N₂O 299.1167, found 299.1160.

BODIPIY 34. According to GP1 using **1b** (25.0 mg, 0.085 mmol), 2-biphenylboronic acid (50.0 mg, 0.255 mmol), Pd₂(dba)₃ (1.0 mg, 2.1 × 10⁻³ mmol), TFP (1.0 mg, 6.3 × 10⁻³ mmol), and CuTC (48.0 mg, 0.2550 mmol). The desired product (32.0 mg, 90%) was obtained as orange crystals. TLC (15% EtOAc/hexanes, R_f = 0.48). Mp: 145–147 °C. IR (KBr, cm⁻¹): 2929 (w), 1566 (s), 1554 (s), 1488 (w), 1434 (w), 1314 (m), 1287 (m), 1140 (s), 1127 (s), 1021 (s), 1002 (s), 982 (m), 746 (m), 720 (w), 700 (w); ¹H NMR (200 MHz, CDCl₃): δ 7.55–7.54 (m, 2H), 7.44–7.42 (m, 2H), 7.26–7.19 (m, 5H), 6.54 (d, J = 4.0 Hz, 2H), 6.19 (d, J = 4.4 Hz, 2H), 3.03–2.97 (m, 4H), 1.28 (t, J = 7.4 Hz, 6H). ¹³C NMR (50 MHz, CDCl₃): δ 163.2, 142.3, 141.9, 140.4, 134.9, 132.6, 131.5, 130.5, 130.2, 129.7, 128.6, 128.4, 127.3, 126.7, 117.1, 22.0, 12.6. HRMS FABS (M + H⁺): calcd for C₂₅H₂₄BF₂N₂ 401.2001, found 401.2005.

BODIPIY 35. According to GP1 using **1b** (10.0 mg, 0.034 mmol), 6-methoxy-2-naphthaleneboronic acid (20.6 mg, 0.102 mmol), Pd₂(dba)₃ (0.8 mg, 8.5 × 10⁻⁴ mmol), TFP (0.6 mg, 2.5 × 10⁻³ mmol), and CuTC (19.4 mg, 0.102 mmol). The desired product (10.8 mg, 79%) was obtained as an orange solid. TLC (20% EtOAc/hexanes, R_f = 0.54). Mp: 185–187 °C. IR (KBr, cm⁻¹): 2973 (w), 1626 (m), 1556 (s), 1491 (s), 1438 (s), 1390 (m), 1319 (s), 1272 (s), 1203 (s), 1147 (s), 1075 (m), 1031 (s), 1009 (s), 987 (s); ¹H NMR (200 MHz, CDCl₃): δ 7.92 (s, 1H), 7.81 (dd, J₁ = 7.8 Hz, J₂ = 2.6 Hz, 2H), 7.57 (dd, J₁ = 8.4 Hz, J₂ = 1.6 Hz, 1H), 7.21 (s, 2H), 6.79 (d, J = 4.0 Hz, 2H), 6.36 (d, J = 4.2 Hz, 2H), 3.97 (s, 3H), 3.09 (q, J = 7.8 Hz, 4H), 1.35 (t, J = 7.6 Hz, 6H). ¹³C NMR (50 MHz, CDCl₃): δ 163.5, 159.1, 143.4, 135.5, 134.7, 130.8, 130.4, 130.3, 129.8, 128.5, 128.3, 126.8, 120.1, 117.4, 105.9, 55.7, 22.3, 13.0. HRMS FABS (M + H⁺): calcd for C₂₄H₂₄BF₂N₂O 405.1950, found 405.1954.

BODIPIY 36. According to GP1 using **1a** (100.0 mg, 0.420 mmol), *p*-tolylboronic acid (171.3 mg, 1.260 mmol), Pd₂(dba)₃ (9.6 mg, 0.011 mmol), TFP (7.3 mg, 0.032 mmol), and CuTC (240.3 mg, 1.260 mmol). The desired product (111.1 mg, 93%) was obtained as orange crystals. ¹H NMR (200 MHz, CDCl₃): δ 7.93 (s, 2H), 7.48 (d, J = 8 Hz, 2H), 7.33 (d, J = 8 Hz, 2H), 6.95 (d, J = 4.2 Hz, 2H), 6.54 (d, J = 3.2 Hz, 2H), 2.48 (s, 3H).⁴⁰

BODIPIY 37. According to GP1 using **1b** (20.0 mg, 0.068 mmol), 1-(phenylsulfonyl)-2-indolylboronic acid (61.4 mg, 0.204 mmol), Pd₂(dba)₃ (1.5 mg, 1.7 × 10⁻³ mmol), TFP (1.2 mg, 5.0 × 10⁻³ mmol), and CuTC (38.8 mg, 0.204 mmol). The desired product (20.5 mg, 60%) was obtained as an orange solid. TLC (15% AcOEt/hexanes

R_f = 0.25). Mp: 176–178 °C. IR (KBr, cm⁻¹): 3158 (w), 3119 (w), 2974 (w), 2937 (w), 2880 (w), 1580 (s), 1559 (s), 1489 (s), 1437 (s), 1376 (s), 1322 (s), 1275 (m), 1187 (m), 1174 (m), 1140 (s), 1089 (m), 1039 (s), 1011 (m), 972 (m), 962 (m), 851 (m), 797 (m), 763 (m), 730 (s), 686 (m), 592 (s), 571 (s), 553 (m). ¹H NMR (200 MHz, CDCl₃): δ 8.10–7.95 (m, 3H), 7.84 (s, 1H), 7.63–7.27 (m, 6H), 6.80 (d, J = 4.2 Hz, 2H), 6.32 (d, J = 4.2 Hz, 2H), 3.09 (q, J = 7.8 Hz, 4H), 1.35 (t, J = 7.4, 6H). ¹³C NMR (50 MHz, CDCl₃): δ 164.2, 138.0, 135.1, 134.6, 134.2, 133.5, 130.6, 129.9, 129.8, 127.9, 127.1, 126.0, 124.3, 121.3, 117.4, 117.1, 113.9, 22.3, 13.0. HRMS FABS (M + H⁺): calcd for C₂₇H₂₅BF₂N₂O₂S 504.1729, found 504.1732.

BODIPIY 38. According to GP1 using **1a** (50.0 mg, 0.210 mmol), 2-fluoro-5-iodophenylboronic acid (167.5 mg, 0.630 mmol), Pd₂(dba)₃ (4.8 mg, 5.2 × 10⁻³ mmol), TFP (3.6 mg, 1.6 × 10⁻³ mmol), and CuTC (119.7 mg, 0.630 mmol). The desired product (53.5 mg, 62%) was obtained as a red solid. TLC (20% EtOAc/hexanes, R_f = 0.46). Mp: 143–145 °C. IR (KBr, cm⁻¹): 3130 (w), 3101 (w), 1569 (s), 1547 (s), 1412 (s), 1387 (s), 1259 (s), 1106 (s), 1071 (s), 1040 (s), 986 (s). ¹H NMR (200 MHz, CDCl₃): δ 7.94 (s, 2H), 7.88–7.74 (m, 2H), 7.03 (t, J = 9.2 Hz, 1H), 6.84 (d, J = 4.0 Hz, 2H), 6.54 (d, J = 4.2 Hz, 2H). ¹³C NMR (50 MHz, CDCl₃): δ 159.7 (d, J = 251.5 Hz), 145.6, 141.3 (d, J = 7.6 Hz), 140.3, 138.4, 135.1, 131.3, 123.9 (d, J = 15.9 Hz), 119.3, 118.7 (d, J = 22.7 Hz), 86.9 (d, J = 3.8 Hz). HRMS FABS (M + H⁺): calcd for C₁₅H₁₀BF₃IN₂ 412.9934, found 412.9933.

BODIPIY 39. According to GP1 using **1b** (25.0 mg, 0.085 mmol) and 1-N-Boc-pyrrole-2-boronic acid (53.0 mg, 0.255 mmol), Pd₂(dba)₃ (1.0 mg, 2.1 × 10⁻³ mmol), TFP (1.0 mg, 6.3 × 10⁻³ mmol), and CuTC (48.0 mg, 0.255 mmol). The desired product (25 mg, 66%) was obtained as red crystals. TLC (15% EtOAc/hexanes, R_f = 0.56). Mp: 130–132 °C. IR (KBr, cm⁻¹): 2972 (w), 2932 (w), 1753 (s), 1561 (s), 1488 (m), 1436 (m), 1308 (s), 1260 (s), 1129 (s), 1054 (s), 1015 (s), 979 (s), 825 (w), 805 (w), 761 (m), 729 (m); ¹H NMR (200 MHz, CDCl₃): δ 7.54–7.51 (m, 1H), 6.78 (d, J = 4.4 Hz, 2H), 6.51–6.48 (m, 1H), 6.36–6.33 (m, 3H), 3.06 (q, J = 7.4 Hz, 4H), 1.34 (t, J = 7.6 Hz, 6H), 1.23 (s, 9H). ¹³C NMR (50 MHz, CDCl₃): δ 163.1, 148.7, 134.7, 129.2, 125.7, 124.9, 119.5, 117.1, 111.1, 85.1, 27.3, 22.1, 13.0. HRMS FABS (M + H⁺): calcd for C₂₂H₂₇BF₂N₂O₂ 414.2164, found 414.2169.

BODIPIY 40. According to GP1 using **1b** (50.0 mg, 0.170 mmol), 4-formylphenylboronic acid (76.0 mg, 0.510 mmol), Pd₂(dba)₃ (3.8 mg, 4.2 × 10⁻³ mmol), TFP (2.9 mg, 0.013 mmol), and CuTC (96.9 mg, 0.510 mmol). The desired product (52.9 mg, 88%) was obtained as an orange solid. TLC (30% EtOAc/hexanes, R_f = 0.60). Mp: 159–160 °C. IR (KBr, cm⁻¹): 3437 (w), 2970 (w), 2925 (w), 1699 (m), 1605 (w), 1572 (s), 1550 (s), 1493 (m), 1436 (m), 1342 (s), 1321 (m), 1275 (m), 1137 (s), 1035 (m), 1008 (m), 978 (m), 804 (w). ¹H NMR (400 MHz, CDCl₃): δ 10.12 (s, 1H), 8.00 (d, J = 8.4 Hz, 2H), 7.66 (d, J = 8.4 Hz, 2H), 6.67 (d, J = 5.1 Hz, 2H), 6.37 (d, J = 4.9 Hz, 2H), 3.08 (dd, J = 16.0, 8.1 Hz, 4H), 1.34 (t, J = 7.8 Hz, 6H). HRMS FABS (M + H⁺): calcd for C₂₀H₂₀BF₂N₂O 353.1637, found 353.1631.

BODIPIY 42. According to GP1 using **1b** (30.0 mg, 0.102 mmol), 4-(trimethylsilyl)phenylboronic acid (59.0 mg, 0.306 mmol), Pd₂(dba)₃ (2.4 mg, 2.6 × 10⁻³ mmol), TFP (1.8 mg, 7.6 × 10⁻³ mmol), and CuTC (58.3 mg, 0.306 mmol). The desired product (39.4 mg, 97%) was obtained as orange crystals. TLC (10% EtOAc/Hexanes, R_f = 0.80). Mp: 160–162 °C. IR (KBr, cm⁻¹): 2966 (w), 1562 (s), 1488 (m), 1402 (w), 1324 (s), 1261 (m), 1131 (s), 1045 (s), 1009 (m), 982 (m), 850 (m). ¹H NMR (200 MHz, CDCl₃): δ 7.62 (d, J = 8.0 Hz, 2H), 7.46 (d, J = 8.0 Hz, 2H), 6.77 (d, J = 4.0 Hz, 2H), 6.34 (d, J = 4.4 Hz, 2H), 3.09 (q, J = 7.5 Hz, 4H), 1.35 (t, J = 7.5 Hz, 6H), 0.33 (s, 9H). ¹³C NMR (50 MHz, CDCl₃): δ 163.7, 143.4, 143.2, 134.8, 134.5, 133.3, 130.8, 129.9, 117.4, 22.3, 13.1, 0.0. HRMS FABS (M + H⁺): calcd for C₂₂H₂₈BF₂N₂Si 397.2083, found 397.2085.

BODIPIY 43. According to GP1 using **1a** (50.0 mg, 0.210 mmol), 2-(methoxycarbonyl)phenylboronic acid (113.4 mg, 0.630 mmol), Pd₂(dba)₃ (4.8 mg, 5.2 × 10⁻³ mmol), TFP (3.6 mg, 1.6 × 10⁻³ mmol), and CuTC (119.7 mg, 0.630 mmol). The desired product (44.0 mg, 65%) was obtained as orange crystals. TLC (15% EtOAc/hexanes, R_f = 0.18). Mp: 135–137 °C. IR (KBr, cm⁻¹): 3117 (w), 1732 (s), 1541 (s), 1388 (s), 1258 (s), 1112 (s), 1075 (vs), 913 (w),

774 (w), 728 (m). ^1H NMR (200 MHz, CDCl_3): δ 8.12–8.08 (m, 1H), 7.93 (s, 2H), 7.68–7.63 (m, 2H), 7.50–7.46 (m, 1H), 6.70–6.68 (m, 2H), 6.50–6.48 (m, 2H), 3.59 (s, 3H). ^{13}C NMR (50 MHz, CDCl_3): δ 166.6, 147.2, 144.1, 135.3, 133.864, 131.9, 131.6, 130.9, 130.7, 130.1, 118.5, 52.4. HRMS FABS ($\text{M} + \text{H}^+$): calcd for $\text{C}_{17}\text{H}_{14}\text{BF}_2\text{N}_2\text{O}_2$ 327.1116, found 327.1119.

BODIPY 44. According to GP1 using **1a** (100.0 mg, 0.420 mmol), 5-formyl-2-methoxyphenylboronic acid (227.0 mg, 1.260 mmol), $\text{Pd}_2(\text{dba})_3$ (9.6 mg, 0.012 mmol), TFP (7.3 mg, 0.031 mmol), and CuTC (339.5 mg, 1.260 mmol). The desired product (128.0 mg, 93%) was obtained as a dark red solid. TLC (30% EtOAc/hexanes R_f = 0.3). Mp: 121–122 °C. IR (KBr, cm^{-1}): 3111 (w), 2930 (w), 2843 (w), 1694 (s), 1599 (s), 1559 (s), 1495 (m), 1412 (s), 1388 (s), 1356 (m), 1261 (s), 1224 (w), 1192 (m), 1179 (m), 1156 (w), 1111 (s), 1075 (s), 1047 (m), 998 (w), 955 (w), 839 (w), 822 (w), 784 (m), 764 (m), 745 (w), 717 (w), 609 (w), 555 (m), 414 (m). ^1H (300 MHz, CDCl_3): δ 9.95 (s, 2H), 8.07 (d, J = 8.4 Hz, 1H), 7.93 (s, 2H), 7.86 (s, 1H), 7.18 (d, J = 8.4 Hz, 1H), 6.75 (s, 2H), 6.51 (s, 2H), 3.86 (s, 3H). ^{13}C NMR (75 MHz, CDCl_3): δ 190.0, 162.1, 144.7, 142.2, 135.6, 133.7, 133.1, 130.9, 129.4, 123.3, 118.7, 111.7, 56.3. HRMS FABS ($\text{M} + \text{H}^+$): calcd for $\text{C}_{17}\text{H}_{14}\text{BF}_2\text{N}_2\text{O}_2$ 327.1116, found 327.1120.

BODIPY 45. According to GP1 using **1a** (50.0 mg, 0.210 mmol), 2-(hydroxymethyl)phenylboronic acid (95.7 mg, 0.630 mmol), $\text{Pd}_2(\text{dba})_3$ (5.0 mg, 5.3×10^{-3} mmol), TFP (3.7 mg, 1.6×10^{-3} mmol), and CuTC (119.7 mg, 0.630 mmol). The desired product (60.1 mg, 94%) was obtained as a bright red solid. TLC (40% acetone/hexanes R_f = 0.4). Mp: 149–150 °C. ^1H (300 MHz, CDCl_3): δ 7.93 (s, 2H), 7.67 (d, J = 7.5 Hz, 1H), 7.56 (t, J = 7.5 Hz, 1H), 7.41 (t, J = 7.5 Hz, 1H), 7.31 (d, J = 7.5 Hz, 1H), 6.71 (s, 2H), 6.50 (s, 2H), 4.58 (s, 2H), 1.75 (s, 1H).⁴¹

BODIPY 46. According to GP1 using **1a** (25.0 mg, 0.105 mmol), benzo[*b*]thien-2-ylboronic acid (56.0 mg, 0.315 mmol), $\text{Pd}_2(\text{dba})_3$ (2.4 mg, 0.003 mmol), TFP (1.8 mg, 0.008 mmol), and CuTC (60.0 mg, 0.315 mmol). The desired product (28.8 mg, 85%) was obtained as red crystals. TLC (15% EtOAc/hexanes R_f = 0.32). Mp: 213–215 °C. IR (KBr, cm^{-1}): 3122 (w), 3064 (w), 1541 (s), 1476 (m), 1411 (s), 1386 (s), 1353 (m), 1261 (s), 1208 (w), 1183 (w), 1158 (w), 1113 (s), 1079 (s), 1040 (s), 966 (m), 935 (w), 892 (w), 872 (w), 808 (w), 769 (m), 744 (m), 731 (w), 628 (w), 597 (w), 549 (w). ^1H NMR (400 MHz, CDCl_3): δ 7.99–7.87 (m, 4H), 7.76 (s, 1H), 7.52–7.43 (m, 2H), 7.32 (d, J = 4.1 Hz, 2H), 6.58 (d, J = 3.7 Hz, 2H). ^{13}C NMR (100 MHz, CDCl_3): δ 144.93, 142.13, 140.19, 139.55, 135.07, 134.76, 132.38, 130.30, 126.95, 125.83, 125.31, 122.58, 119.20. HRMS FABS ($\text{M} + \text{H}^+$): calcd for $\text{C}_{17}\text{H}_{12}\text{BF}_2\text{N}_2\text{S}$ 325.0782, found 325.0786.

General Procedure for the L–S Cross-Coupling with Boronic Acids under Microwave Irradiation (GP2). A thick-walled tube equipped with a stir bar was charged with **1a** (1 equiv), the corresponding boronic acid (3 equiv), and dry THF (3 mL). The mixture was sparged with N_2 for 5 min whereupon $\text{Pd}_2(\text{dba})_3$ (2.5 mol %), trifurylphosphine (7.5%), and CuTC (3 equiv) were added under N_2 . The tube was sealed and heated under microwave irradiation at 100 °C (200 psi, 150 W) for the corresponding reaction time (see Table 1). After the reaction mixture reached rt, the crude material was adsorbed in SiO_2 gel, and the product was purified by flash chromatography on SiO_2 gel using EtOAc/hexanes gradients. For the purpose of characterization, the products were crystallized from CH_2Cl_2 /petroleum ether.

BODIPY 33. According to GP2 using **1a** (50.0 mg, 0.210 mmol), 3-(hydroxymethyl)phenylboronic acid (95.7 mg, 0.630 mmol), $\text{Pd}_2(\text{dba})_3$ (5.0 mg, 5.3×10^{-3} mmol), TFP (3.7 mg, 1.6×10^{-3} mmol), and CuTC (119.7 mg, 0.630 mmol). The desired product (59.4 mg, 95%) was obtained as a red solid. Characterization data is given above.

BODIPY 12. According to GP2 using **1a** (25 mg, 0.105 mmol), 2-bromophenylboronic acid (63 mg, 0.315 mmol), $\text{Pd}_2(\text{dba})_3$ (2.4 mg, 0.003 mmol), TFP (1.8 mg, 0.008 mmol), and CuTC (60 mg, 0.315 mmol). The desired product (31 mg, 85%) was obtained as orange crystals. Mp: 150–152 °C. ^1H NMR (200 MHz, CDCl_3): δ 7.95 (s, 2H), 7.76–7.71 (m, 1H), 7.47–7.37 (m, 3H), 6.72 (d, J = 4.0, 2H), 6.51 (d, J = 4.4, 2H).¹⁹

BODIPY 31. According to GP2 using **1a** (25 mg, 0.105 mmol), 4-chlorophenylboronic acid (49 mg, 0.315 mmol), $\text{Pd}_2(\text{dba})_3$ (2.4 mg, 0.003 mmol), TFP (1.8 mg, 0.008 mmol), and CuTC (60 mg, 0.315 mmol). The desired product (28 mg, 90%) was obtained as an orange-reddish solid. Characterization data is given above.

BODIPY 4. According to GP2 using **1a** (25 mg, 0.105 mmol), 4-biphenylboronic acid (62 mg, 0.315 mmol), $\text{Pd}_2(\text{dba})_3$ (2.4 mg, 0.003 mmol), TFP (1.8 mg, 0.008 mmol), and CuTC (60 mg, 0.315 mmol). The desired product (33 mg, 92%) was obtained as orange-red crystals. Mp: 212–213 °C. ^1H NMR (200 MHz, CDCl_3): δ 7.96 (s, 2H), 7.78–7.639 (m, 6H), 7.55–7.425 (m, 3H), 7.03 (d, J = 4 Hz, 2H), 6.57 (d, J = 2.8 Hz, 2H).¹⁹

BODIPY 8. According to GP2 using **1a** (25 mg, 0.105 mmol), 4-methoxyphenylboronic acid (48 mg, 0.315 mmol), $\text{Pd}_2(\text{dba})_3$ (2.4 mg, 0.003 mmol), TFP (1.8 mg, 0.008 mmol), and CuTC (60 mg, 0.315 mmol). The desired product (28 mg, 91%) was obtained as orange crystals. Mp: 137–138 °C. ^1H NMR (200 MHz, CDCl_3): δ 7.92 (s, 2H), 7.55 (dt, J_1 = 8.8 Hz, J_2 = 2.1 Hz, 2H), 7.05 (dt, J_1 = 9.0 Hz, J_2 = 2.2 Hz, 2H), 6.98 (d, J = 4.0 Hz, 2H), 6.56–6.54 (m, 2H), 3.92 (s, 3H).¹⁹

General Procedure for the L–S Cross-Coupling with Organostannanes Using Cu(I) Phosphinate as Cu(I) Source (GP3). A Schlenk tube was charged under N_2 with dry THF (2 mL), methylthiobodipy **1a** (1 equiv), the organostannane (3 equiv), $\text{Pd}(\text{PPh}_3)_4$ (5%), and Cu(I) phosphinate (3 equiv). Then the reaction flask was immersed into a preheated oil bath at 55 °C. The reaction progress was followed by TLC (SiO_2 gel, 20% EtOAc/hexanes). After the starting material was consumed, the mixture was allowed to cool to rt, and the solvent was removed in vacuo. The product was obtained after flash chromatography (SiO_2 gel, EtOAc/hexanes gradient) followed by crystallization in petroleum ether.

BODIPY 8. According to GP3 using **1a** (25 mg, 0.105 mmol), (4-methoxyphenyl)tributylstannane (125 mg, 0.315 mmol), $\text{Pd}(\text{PPh}_3)_4$ (6.0 mg, 5 mol %), and CuOP(O)Ph₂ (88 mg, 0.315 mmol). The desired product (26 mg, 85%) was obtained as orange crystals. Mp: 137–138 °C. ^1H NMR (200 MHz, CDCl_3): δ 7.92 (s, 2H), 7.55 (dt, J_1 = 8.8 Hz, J_2 = 2.1 Hz, 2H), 7.05 (dt, J_1 = 9.0 Hz, J_2 = 2.2 Hz, 2H), 6.98 (d, J = 4.0 Hz, 2H), 6.56–6.54 (m, 2H), 3.92 (s, 3H).¹⁹

BODIPY 36. According to GP3 using **1a** (25 mg, 0.105 mmol), (4-methylphenyl)tributylstannane (120 mg, 0.315 mmol), $\text{Pd}(\text{PPh}_3)_4$ (6.0 mg, 5 mol %), and CuOP(O)Ph₂ (88 mg, 0.315 mmol). The desired product (23 mg, 77%) was obtained as orange crystals. ^1H NMR (200 MHz, CDCl_3): δ 7.93 (s, 2H), 7.48 (d, J = 8 Hz, 2H), 7.33 (d, J = 8 Hz, 2H), 6.95 (d, J = 4.2 Hz, 2H), 6.54 (d, J = 3.2 Hz, 2H), 2.48 (s, 3H).⁴⁰

BODIPY 31. According to GP3 using **1a** (25 mg, 0.105 mmol), (4-chlorophenyl)tributylstannane (126 mg, 0.315 mmol), $\text{Pd}(\text{PPh}_3)_4$ (6.0 mg, 5 mol %), and CuOP(O)Ph₂ (88 mg, 0.315 mmol). The desired product (26 mg, 81%) was obtained as orange-reddish solid. Characterization data are given above.

BODIPY 48. According to GP3 using **1a** (25 mg, 0.105 mmol), 3-(1,3-benzodioxole)tributylstannane (129 mg, 0.315 mmol), $\text{Pd}(\text{PPh}_3)_4$ (6.0 mg, 5 mol %), and CuOP(O)Ph₂ (88 mg, 0.315 mmol). The desired product (25 mg, 75%) was obtained as a red solid. TLC (25% EtOAc/hexanes R_f = 0.31). Mp: 133–134 °C. IR 3117 (m), 2901 (bs), 1551 (bs), 1412 (s), 1388 (s), 1263 (s), 1254 (s), 1117 (s), 1079 (s), 1044 (s). ^1H NMR (CDCl_3): δ = 6.11 (2, s), 6.55 (2, bd, J = 3.2), 6.94–7.02 (3, m), 7.08–7.14 (2, m), 7.92 (2, bs). ^{13}C NMR (CDCl_3): δ = 102.1, 108.7, 111.1, 118.6, 125.8, 127.9, 131.5, 135.1, 144.0, 147.2, 148.2, 150.5. HRMS FABS ($\text{M} + \text{H}^+$): calcd for $\text{C}_{16}\text{H}_{12}\text{BF}_2\text{N}_2\text{O}_2$ 313.0960, found 313.0959.

BODIPY 2. According to GP3 using **1a** (25 mg, 0.105 mmol), phenyltributylstannane (115 mg, 0.315 mmol), $\text{Pd}(\text{PPh}_3)_4$ (6.0 mg, 5 mol %), and CuOP(O)Ph₂ (88 mg, 0.315 mmol). The desired product (25 mg, 90%) was obtained as orange crystals. ^1H NMR (200 MHz, CDCl_3): δ 7.95 (s, 2H), 7.61–7.53 (m, 5 H), 6.94 (d, J = 4.4 Hz, 2.0 H), 6.55 (d, J = 3.8 Hz, 2H).²²

■ ASSOCIATED CONTENT

■ Supporting Information

Copies of the ^1H and ^{13}C NMR spectra of all the compounds described and full photophysical data. The Supporting Information is available free of charge on the ACS Publications website at DOI: 10.1021/acs.joc.5b00731.

■ AUTHOR INFORMATION

Corresponding Authors

*E-mail: jorge.banuelos@ehu.es.

*E-mail: eduardop@ugto.mx.

Notes

The authors declare no competing financial interest.

■ ACKNOWLEDGMENTS

We thank CONACyT (Grant Nos. 129572 and 123732), DAIP-UG 2014, MINECO (MAT2014-51937-C3-3), and Gobierno Vasco (IT339-10) for financial support. B.Z.T. thanks the Hong Kong Research Grants Council (Project No. 603008). We also thank Cuantico de Mexico (www.cuantico.mx) for the kind donation of BODIPYs **1a,b**.

■ REFERENCES

- (1) (a) BODIPYs are a registered trademark of Molecular Probes Inc., Eugene, OR. (b) Haugland, R. P. *The Molecular Probes Handbook. A Guide to Fluorescent Probes and Labeling Technologies*, 10th ed.; Molecular Probes, Inc.: Eugene, OR, 2010.
- (2) Treibs, A.; Kreuzer, F.-H. *Liebigs Ann. Chem.* **1968**, *718*, 208.
- (3) (a) Ziessel, R.; Ulrich, G.; Harriman, A. *New J. Chem.* **2007**, *31*, 496. (b) Ulrich, G.; Ziessel, R.; Harriman, A. *Angew. Chem., Int. Ed.* **2008**, *47*, 1184. (c) Benniston, A. C.; Copley, G. *Phys. Chem. Chem. Phys.* **2009**, *11*, 4124. (d) Loudet, A.; Burgess, K. *Chem. Rev.* **2007**, *107*, 4891. (e) Wood, T. E.; Thompson, A. *Chem. Rev.* **2007**, *107*, 1831.
- (4) (a) West, R.; Panagabko, C.; Atkinson, J. *J. Org. Chem.* **2010**, *75*, 2883. (b) Ehrenschröder, T.; Wagenknecht, H.-A. *Synthesis* **2008**, 3657.
- (5) (a) Rio, Y.; Seitz, W.; Gouloumis, A.; Vazquez, P.; Sessler, J. L.; Guldi, D. M.; Torres, T. *Chem.—Eur. J.* **2010**, *16*, 1929. (b) Koepf, M.; Trabolsi, A.; Elhabiri, M.; Wytko, J. A.; Paul, D.; Albrecht-Gary, A. M.; Weiss, J. *Org. Lett.* **2005**, *7*, 1279.
- (6) Lee, C. Y.; Hupp, J. T. *Langmuir* **2010**, *26*, 3760.
- (7) (a) Rao, M. R.; Mobin, S. M.; Ravikanth, M. *Tetrahedron* **2010**, *66*, 1728. (b) Vendrell, M.; Krishna, G. G.; Ghosh, K. K.; Zhai, D.; Lee, J.-S.; Zhu, Q.; Yau, Y. H.; Geifman Shochat, S.; Kim, H.; Chung, J.; Chang, Y.-T. *Chem. Commun.* **2011**, *47*, 8424. (c) Boens, N.; Qin, W.; Baruah, M.; De Borggraeve, W. M.; Filarowski, A.; Smisdom, N.; Ameloot, M.; Crovotto, L.; Talavera, E. M.; Alvarez-Pez, J. M. *Chem.—Eur. J.* **2011**, *17*, 10924. (d) Boens, N.; Leen, V.; Dehaen, W. *Chem. Soc. Rev.* **2012**, *41*, 1130. (e) Cheng, T.; Wang, T.; Zhu, W.; Yang, Y.; Zeng, B.; Xu, Y. *Chem. Commun.* **2011**, *47*, 3915.
- (8) Godoy, J.; Vives, G.; Tour, J. M. *Org. Lett.* **2010**, *12*, 1464.
- (9) Lu, J.; Fu, H.; Zhang, Y.; Jakubek, Z. J.; Tao, Y.; Wang, S. *Angew. Chem., Int. Ed.* **2011**, *50*, 11658.
- (10) Baker, J. G.; Adams, L. A.; Salchow, K.; Mistry, S. N.; Middleton, R. J.; Hill, S. J.; Kellam, B. *J. Med. Chem.* **2011**, *54*, 6874.
- (11) Bura, T.; Leclerc, N.; Fall, S.; Léveque, P.; Heiser, T.; Ziessel, R. *Org. Lett.* **2011**, *13*, 6030.
- (12) Kim, D.-R.; Ahn, H.-C.; Lee, W.-J.; Ahn, D.-R. *Chem. Commun.* **2011**, *47*, 791.
- (13) Kang, N.-Y.; Lee, S.-C.; Park, S.-J.; Ha, H.-H.; Yun, S.-W.; Kostromina, E.; Gustavsson, N.; Ali, Y.; Chandran, Y.; Chun, H.-S.; Bae, M.; Ahn, J. H.; Han, W.; Radda, G. K.; Chang, Y.-T. *Angew. Chem., Int. Ed.* **2013**, *52*, 8557.
- (14) Xu, W.; Bai, J.; Peng, J.; Samanta, A.; Divyanshu; Chang, Y.-T. *Chem. Commun.* **2014**, *50*, 10398.

- (15) (a) Chen, J.; Burghart, A.; Derecskei-Kovacs, A.; Burgess, K. *J. Org. Chem.* **2000**, *65*, 2900. (b) Thorensen, L. H.; Kim, H.; Welch, M. B.; Burghart, A.; Burgess, K. *Synlett* **1998**, 1276. (c) Goze, C.; Ulrich, G.; Ziessel, R. *Org. Lett.* **2006**, *8*, 4445. (d) Gose, C.; Ulrich, G.; Mallon, L. J.; Allen, B. D.; Harriman, A.; Ziessel, R. *J. Am. Chem. Soc.* **2006**, *128*, 10231. (e) Goze, C.; Ulrich, G.; Ziessel, R. *J. Org. Chem.* **2007**, *72*, 313. (f) Rohland, T.; Baruah, M.; Qin, W.; Boens, N.; Dehaen, W. *Chem. Commun.* **2006**, 266. (g) Rohland, T.; Qin, W.; Boens, N.; Dehaen, W. *Eur. J. Org. Chem.* **2006**, 4658. (h) Tahtaoui, C.; Thomas, C.; Rohmer, F.; Klotz, P.; Duportail, G.; Mely, Y.; Bonnet, D.; Hibert, M. *J. Org. Chem.* **2007**, *72*, 269. (i) Dost, Z.; Atilgan, S.; Akkaya, E. U. *Tetrahedron* **2006**, *62*, 8484. (j) Yu, Y.-H.; Descalzo, A. B.; Shen, Z.; Röhr, H.; Liu, Q.; Wang, Y.-W.; Spieles, M.; Li, Y.-Z.; Rurack, K.; You, X.-Z. *Chem.—Asian J.* **2006**, *1*–2, 176. (k) Lee, J.-S.; Kang, N.-y.; Kim, Y. K.; Samanta, A.; Feng, S.; Kim, H. K.; Vendrell, M.; Park, J. H.; Chang, Y.-T. *J. Am. Chem. Soc.* **2009**, *131*, 10077. (l) Hayashi, Y.; Yamaguchi, S.; Cha, W. Y.; Kim, D.; Shinokubo, H. *Org. Lett.* **2011**, *13*, 2992. (m) Komatsu, T.; Urano, Y.; Fujikawa, Y.; Kobayashi, T.; Kojima, H.; Terai, T.; Hanaokaa, K.; Nagano, T. *Chem. Commun.* **2009**, 7015. (n) Zheng, Q.; He, G. S.; Prasad, P. N. *Chem. Phys. Lett.* **2009**, *475*, 250. (o) Bozdemir, Ö. A.; Büyükcakir, O.; Akkaya, E. U. *Chem.—Eur. J.* **2009**, *15*, 3830. (p) Ikeda, C.; Ueda, S.; Nabeshima, T. *Chem. Commun.* **2009**, 2544. (q) Li, X.; Huang, S.; Hu, Y. *Org. Biomol. Chem.* **2012**, *10*, 2369. (r) Khan, T. K.; Pissurlenkar, R. R. S.; Shaikh, M. S.; Ravikanth, M. *J. Organomet. Chem.* **2012**, *697*, 65. (s) Leen, V.; Leemans, T.; Boens, N.; Dehaen, W. *Eur. J. Org. Chem.* **2011**, 4386. (t) Jiang, X.-D.; Zhang, J.; Furuyama, T.; Zhao, W. *Org. Lett.* **2012**, *14*, 248. (u) Wu, W.; Guo, H.; Wu, W.; Ji, S.; Zhao, J. *J. Org. Chem.* **2011**, *76*, 7056. (v) Verbelen, B.; Leen, V.; Wang, L.; Boens, N.; Dehaen, W. *Chem. Commun.* **2012**, *48*, 9129. (w) Yokoi, H.; Wachi, N.; Hiroto, S.; Shinokubo, H. *Chem. Commun.* **2014**, *50*, 2715.
- (16) Ueno, T.; Urano, Y.; Kojima, H.; Nagano, T. *J. Am. Chem. Soc.* **2006**, *128*, 10640.
- (17) Bañuelos, J.; Arroyo-Córdoba, I. J.; Valois-Escamilla, I.; Alvarez-Hernández, A.; Peña-Cabrera, E.; Hu, R.; Tang, B. Z.; Esnal, I.; Martínez, V.; López Arbeloa, I. *RSC Adv.* **2011**, *1*, 677.
- (18) (a) Pochorovski, I.; Breiten, B.; Schweizer, W. B.; Diederich, F. *Chem.—Eur. J.* **2010**, *16*, 12590. (b) Alamiry, M. A. H.; Benniston, A. C.; Copley, G.; Harriman, A.; Howgego, D. *J. Phys. Chem. A* **2011**, *115*, 12111. (c) Röhr, H.; Trieflinger, C.; Rurack, K.; Daub, J. *Chem.—Eur. J.* **2006**, *12*, 689. (d) Yu, H.; Xiao, Y.; Guo, H.; Qian, X. *Chem.—Eur. J.* **2011**, *17*, 3179. (e) Wüstner, D.; Solankoa, L.; Sokola, E.; Garvikb, O.; Li, Z.; Bittmann, R.; Korted, T.; Herrmann, A. *Chem. Phys. Lip.* **2011**, *164*, 221. (f) Dumas-Verdes, C.; Miomandre, F.; Lépiciere, E.; Galangau, O.; Vu, T. V.; Clavier, G.; Méallet-Renault, R.; Audebert, P. *Eur. J. Org. Chem.* **2010**, 2525. (g) Lazarides, T.; McCormick, T. M.; Wilson, K. C.; Lee, S.; McCamant, D. W.; Eisenberg, R. *J. Am. Chem. Soc.* **2011**, *133*, 350. (h) Dodani, S. C.; Leary, S. C.; Cobine, P. A.; Winge, D. N.; Chang, C. J. *J. Am. Chem. Soc.* **2011**, *133*, 8606. (i) Ehrenschröder, T.; Wagenknecht, H.-A. *J. Org. Chem.* **2011**, *76*, 2301. (j) Liras, M.; García, O.; Quijada-Garrido, I.; París, R. *Macromolecules* **2011**, *44*, 1335. (k) Kim, T.-I.; Park, J.; Park, S.; Choi, Y.; Kim, Y. *Chem. Commun.* **2011**, *47*, 12640. (l) Whited, M. T.; Patel, N. M.; Roberts, S. T.; Allen, K.; Djurovich, P. I.; Bradforth, S. E.; Thompson, M. E. *Chem. Commun.* **2012**, *48*, 284. (m) Murale, D. P.; Lee, K. M.; Kima, K.; Churchill, D. G. *Chem. Commun.* **2011**, *47*, 12512. (n) Baruah, M.; Qin, W.; Basaric, N.; De Borggraeve, W. M.; Boens, N. *J. Org. Chem.* **2005**, *70*, 4152. (o) Chen, Y.; Zhao, J.; Guo, H.; Xie, L. *J. Org. Chem.* **2012**, *77*, 2192. (p) Matsumoto, T.; Urano, Y.; Shoda, T.; Kojima, H.; Nagano, T. *Org. Lett.* **2007**, *9*, 3375. (q) Kamiya, M.; Johnsson, K. *Anal. Chem.* **2010**, *82*, 6472. (r) Lee, C.-H.; Yoon, H.-J.; Shim, J.-S.; Jang, W.-D. *Chem.—Eur. J.* **2012**, *18*, 4513. (s) Lu, H.; Zhang, S.; Liu, H.; Wang, Y.; Shen, Z.; Liu, C.; You, X. *J. Phys. Chem. A* **2009**, *113*, 14081. (t) Rosenthal, J.; Lippard, S. J. *J. Am. Chem. Soc.* **2010**, *132*, 5536. (u) Nierth, A.; Kobitski, A. Y.; Nienhaus, G. U.; Jäschke, A. *J. Am. Chem. Soc.* **2010**, *132*, 2646. (v) Bozdemir, O. A.; Sozmen, F.; Buyukcakir, O.; Guliyev, R.; Cakmak, Y.; Akkaya, E. U. *Org. Lett.* **2010**, *12*, 1400. (w) Dodani, S. C.; He, Q.; Chang, C. J. *J.*

- Am. Chem. Soc.* **2009**, *131*, 18020. (x) Saito, R.; Ohno, A.; Ito, E. *Tetrahedron* **2010**, *66*, 583. (y) Peña, B.; Barhoumi, R.; Burghardt, R. C.; Turro, C.; Dunbar, K. R. *J. Am. Chem. Soc.* **2014**, *136*, 7861.
- (19) Peña-Cabrera, E.; Aguilar-Aguilar, A.; Gonzalez-Dominguez, M.; Lager, E.; Zamudio-Vazquez, R.; Godoy-Vargas, J.; Villanueva-García, F. *Org. Lett.* **2007**, *9*, 3985.
- (20) (a) H. Prokopcová, H.; Kappe, C. O. *Angew. Chem., Int. Ed.* **2008**, *47*, 3674. (b) Prokopcová, H.; Kappe, C. O. *Angew. Chem., Int. Ed.* **2009**, *48*, 2276.
- (21) Goud, T. V.; Tutar, A.; Biellmann, J.-F. *Tetrahedron* **2006**, *62*, 5084.
- (22) Wagner, R. W.; Lindsey, J. S. *Pure Appl. Chem.* **1996**, *68*, 1373.
- (23) (a) Lager, E.; Liu, J.; Aguilar-Aguilar, A.; Tang, B. Z.; Peña-Cabrera, E. *J. Org. Chem.* **2009**, *74*, 2053. (b) Arroyo, I. J.; Hu, R.; Tang, B. Z.; López, F. I.; Peña-Cabrera, E. *Tetrahedron* **2011**, *67*, 7244.
- (24) Arroyo, I. J.; Hu, R.; Merino, G.; Tang, B. Z.; Peña-Cabrera, E. *J. Org. Chem.* **2009**, *74*, 5719.
- (25) Esnal, I.; Urías-Benavides, A.; Gómez-Durán, C. F. A.; Osorio-Martínez, C. A.; García-Moreno, I.; Costela, A.; Bañuelos, J.; Epelde, N.; López Arbeloa, I.; Hu, R.; Tang, B. Z.; Peña-Cabrera, E. *Chem.—Asian J.* **2013**, *8*, 2691.
- (26) Flores-Rizo, J. O.; Esnal, I.; Osorio-Martínez, C. A.; Gómez-Durán, C. F. A.; Bañuelos, J.; López Arbeloa, I.; Pannell, K. H.; Metta-Magaña, A. J.; Peña-Cabrera, E. *J. Org. Chem.* **2013**, *78*, 5867.
- (27) Gutiérrez-Ramos, B. D.; Bañuelos, J.; Arbeloa, T.; López Arbeloa, I.; González-Navarro, P. E.; Wrobel, K.; Cerdán, L.; García-Moreno, I.; Costela, A.; Peña-Cabrera, E. *Chem.—Eur. J.* **2015**, *21*, 1755.
- (28) Martínez-Gonzalez, M. R.; Urías-Benavides, A.; Alvarado-Martínez, E.; Lopez, J. C.; Gómez, A. M.; del Rio, M.; Garcia, I.; Costela, A.; Bañuelos, J.; Arbeloa, T.; Lopez Arbeloa, I.; Peña-Cabrera, E. *Eur. J. Org. Chem.* **2014**, *26*, 5659.
- (29) Kinzel, T.; Zhang, Y.; Buchwald, S. L. *J. Am. Chem. Soc.* **2010**, *132*, 14073.
- (30) (a) Gräf, K.; Körzdörfer, T.; Kümmel, S.; Thelakkat, M. *New J. Chem.* **2013**, *37*, 1417. (b) Barin, G.; Yilmaz, M. D.; Akkaya, E. U. *Tetrahedron Lett.* **2009**, *50*, 1738. (c) Erten-Ela, S.; Yilmaz, M. D.; Icli, B.; Dede, Y.; Icli, S.; Akkaya, E. U. *Org. Lett.* **2008**, *10*, 3299.
- (31) Yue, Y.; Guo, Y.; Xua, J.; Shao, S. *New J. Chem.* **2011**, *35*, 61.
- (32) Roacho, R. I.; Metta-Magaña, A.; Peña-Cabrera, E.; Pannell, K. *Org. Biomol. Chem.* **2015**, *13*, 995.
- (33) (a) Egi, M.; Liebeskind, L. S. *Org. Lett.* **2003**, *5*, 801. (b) Li, H.; Yang, H.; Liebeskind, L. S. *Org. Lett.* **2008**, *10*, 4375.
- (34) Mee, S. P. H.; Lee, V.; Baldwin, J. E. *Angew. Chem., Int. Ed.* **2004**, *43*, 1132.
- (35) Alphonse, F.-A.; Suzenet, F.; Keromnes, A.; Lebret, B.; Guillaumet, G. *Org. Lett.* **2003**, *5*, 803.
- (36) Duran-Sampedro, G.; Agarrabeitia, A. R.; Garcia-Moreno, I.; Costela, A.; Bañuelos, J.; Arbeloa, T.; López Arbeloa, I.; Chiara, J. L.; Ortiz, M. J. *Eur. J. Org. Chem.* **2012**, 6335.
- (37) Gibbs, J. H.; Robins, L. T.; Zhou, Z.; Bobadova-Parvanova, P.; Cottam, M.; McCandless, G. T.; Fronczek, F. R.; Vicente, M. G.H. *Bioorg. Med. Chem.* **2013**, *21*, 5770.
- (38) (a) Kuimova, M. K.; Botchway, S. W.; Parker, A. W.; Balaz, M.; Collins, H. A.; Anderson, H. L.; Suhling, K.; Ogilby, P. R. *Nat. Chem.* **2009**, *1*, 69. (b) Kuimova, M. K.; Yahioğlu, G.; Levitt, J. A.; Suhling, K. *J. Am. Chem. Soc.* **2008**, *130*, 6672. (c) Alamiry, M. A. H.; Benniston, A. C.; Copley, G.; Elliot, K. J.; Harriman, A.; Stewart, B.; Zhi, Y.-G. *Chem. Mater.* **2008**, *20*, 4024.
- (39) Swamy, P. C. A.; Thilagar, P. *Inorg. Chim. Acta* **2014**, *411*, 97.
- (40) Cui, A.; Peng, X.; Fan, J.; Chen, X.; Wu, Y.; Guo, B. *J. Photochem. Photobiol. A* **2007**, *186*, 85.
- (41) Roacho, R. I.; Metta-Magaña, A. J.; Peña-Cabrera, E.; Pannell, K. *H. J. Phys. Org. Chem.* **2013**, *26*, 345.